RESEARCH ARTICLE

physica
pss
status
solidi
a

www.pss-a.com

A Power Loss-Based Modeling of Power Conversion Efficiency in Organic and Perovskite Solar Cells

Hooman Mehdizadeh-Rad, Daniel Dodzi Yao Setsoafia, Kiran Sreedhar Ram, Mojtaba Abdi-Jalebi, David Ompong, and Jai Singh*

This article presents a new mathematical model for simulating the power conversion efficiency (PCE) of organic solar cells (OSCs) and perovskite solar cells (PSCs). This model incorporates all power losses that can occur before the charge carriers are collected by their respective electrodes. This includes power loss due to thermalization of the charge carriers above the bandgap ($P_{Thermal}$), charge carrier recombination (P_{rec}), dissociation of excitons (P_{BI}), and the transport of free charge carriers to their respective electrodes through the energy off-sets (P_B). By quantifying each power loss, the model can simulate the net electrical power generated by a solar cell and estimate its PCE. The validity of the mathematical model is tested by comparing the calculated PCE of an OSC and a PSC with their experimental results and the results obtained from the conventional simulation, which are found to be in good agreement. It is found that the highest power loss occurs due to $P_{Thermal}$ in both OSC and PSC. Compared to conventional models, this model establishes a direct relationship between PCE and individual power losses that may occur in both OSCs and PSCs.

1. Introduction

Solar cells play a crucial role in transforming solar energy into electricity, which makes them a promising solution to meet the ever-increasing demand for clean energy while reducing

H. Mehdizadeh-Rad, D. D. Y. Setsoafia, K. Sreedhar Ram, D. Ompong, J. Singh
Faculty of Science and Technology
Charles Darwin University
Darwin 0909, NT, Australia
E-mail: jai.singh@cdu.edu.au

H. Mehdizadeh-Rad, D. Ompong, J. Singh
Energy and Resources Institute
Charles Darwin University
Darwin 0909, NT, Australia

M. Abdi-Jalebi
Institute for Materials Discovery
University College London
Malet Place, London WC1E 7JE, UK

harmful carbon emissions.[1] In recent years, there has been a growing interest in the development of efficient and cost-effective solar cells to meet the increasing demand for clean energy. Among various types of solar cells, perovskite solar cells (PSCs) and organic solar cells (OSCs) have garnered significant research attention for their favorable photovoltaic properties.[2] PSCs and OSCs offer advantages such as low-cost material constituents and simple fabrication processes.[3] Currently, the highest reported power conversion efficiency (PCE) for OSCs is 19.31[4] and for PSCs over 26.1%.[5] However, both technologies are still undergoing rapid development in their device architecture and materials formulations, and future advancements may further increase their efficiency. PCE of OSCs and PSCs can be determined by measuring their current–voltage (I–V) curves experimentally. In addition to experimental measurement, computer simulations and modeling can also be used to predict and optimize PCE of OSCs and PSCs. To simulate the PCE of OSCs and PSCs, the optical and electrical mathematical models are developed. Among the various optical models developed in the literature,[6] the mathematical model developed by Pettersson et al.[7] using the transfer matrix method is the most commonly used. The electrical mathematical models are developed using Poisson's and drift-diffusion equations.[8] The numerical solution of the drift-diffusion equations typically involves the use of the finite difference method, whereby the differential equations are discretized on a finite set of points and solved either by the Scharfetter–Gummel discretization scheme[9] or Newton's iteration method.[8a,10]

Usually, one simulates PCE of a solar cell by determining fill factor (FF), open circuit voltage (V_{oc}), and short circuit current (J_{sc}),[11] however, except FF that is related directly to the maximum electrical power output, none of the other two parameters directly plays any role in PCE[12]. Moreover, in this approach, a full account of different energy losses and heat sources on PCE is not fully accepted. Some examples of such losses include the heat generated by the thermalization of charge carriers produced by the absorption of photons with energy greater than the bandgap energy, recombination in tail states, and vibrational energy required for the dissociation of charge transfer (CT) excitons at the donor–acceptor interfaces, as well as the transfer of charge carriers through the energy offsets at interfaces.[13] It may be

noted that by incorporating these losses in the simulation, one can better understand the factors that may be used to maximize PCE in OSCs and PSCs.

Therefore, this article proposes an alternative methodology for simulating PCE of OSCs and PSCs that incorporates heat transfer mechanisms. It incorporates different heat sources affecting PCE of a solar cell, such as the total power loss due to thermalization of charge carriers, recombination of photo-generated electron and hole pairs, the thermal power loss due to the transport of free charge carriers to their respective electrodes through energy off-sets, and the vibrational energy required for the dissociation of CT excitons at the donor–acceptor interfaces. By considering these factors, the proposed model may help quantify and understand the influence of different heat transfer factors on PCE of OSCs and PSCs.

This study is expected to be the first attempt to introduce a model that considers heat transfer in simulating PCE in OSCs and PSCs. The outcomes of this article may be expected to aid in improving the design and performance of these solar cells.

2. Methodology

PCE of a solar cell is usually defined as the ratio of the net maximum electrical power output to the total incident power of irradiation and usually written as

$$\text{PCE} = \frac{P_{\text{net-max}}^{\text{Elect}}}{IrA} \tag{1}$$

where $P_{\text{net-max}}^{\text{Elect}}$ (W) is the net maximum electrical power output obtained from the maximum power point on the J–V characteristics, Ir is the incident solar radiation (W m^{-2}), and A is the solar cell area (m^2).

When photons are absorbed in the active layer of a solar cell, depending on the energy of photons, some electrons may be excited from the valence band or highest occupied molecular orbital (HOMO) for OSCs to energies higher than the conduction band or lowest unoccupied molecular orbital (LUMO) for OSCs and some may exactly to the conduction band. Thus, the total solar power absorbed can be written as, $P_{\text{abs}} = Ir\alpha A$, where α is the absorbance of the active layer in an OSC or a PSC. The electrons excited by photons of energy higher than the bandgap energy will first relax down to the edge of the conduction band (LUMO) by losing the excess energy, usually called the thermalization of charge carriers. The power loss by thermalization, P_{Thermal}, of such charge carriers can be written as:[13]

$$P_{\text{Thermal}} = Ir\alpha A - P_{\text{G}} \tag{2}$$

where P_{G} is the solar power required to excite electrons exactly from the valence band (HOMO) to the conduction band (LUMO), and it can be obtained as:[14]

$$P_{\text{G}} = qGE_{\text{g}}Ad \tag{3}$$

where q (C) is the electric charge, G (s^{-1} m^{-3}) is the rate of total electron–hole pair generation, which can be determined by the optical transfer matrix method,[7] E_{g} (eV) is bandgap energy, and d (m) is active layer thickness.[8b,14]

The net maximum electrical power output, $P_{\text{net-max}}^{\text{Elect}}$, in a solar cell can be obtained by accounting the various sources of power loss as described below.

Some of the electrons and holes generated may recombine radiatively and nonradiatively by causing a power loss denoted by P_{rec}, which can be written as:[14]

$$P_{\text{rec}} = qRE_{\text{g}}Ad \tag{4}$$

where R (s^{-1} m^{-3}) is the total recombination rate, which can be calculated using drift-diffusion equations,[8b] including radiative (Langevin recombination[15]) and nonradiative recombination (tail state recombination[15b,16]).

In addition, some charge carriers may lose power, denoted by P_{B}, by moving to lower energy due to energy off-sets while transferring toward their respective electrodes. We can calculate the power loss P_{B} as:

$$P_{\text{B}} = q(G - R)BAd \tag{5}$$

where B is the total energy off-set and can be written as (see **Figure 1** and **2**)

$$B = B_{\text{a}} + B_{\text{c}} \tag{6}$$

where B_{a} (eV) is the energy off-set between the anode and active layer, and B_{c} (eV) is the energy offset between the cathode and the active layer. Finally, power loss due to the dissociation of CT excitons at the donor–acceptor interface, denoted by P_{BI} is nonzero in OSCs due to higher exciton binding energy but almost zero in PSCs as the excitons are dissociated with very low energy due to the high dielectric constant. Thus, P_{BI} for OSCs can be determined by:

$$P_{\text{BI}} = q(G - R)(B_{\text{IL}} + B_{\text{IH}})Ad \tag{7}$$

where B_{IL}(eV) is the energy off-set between LUMOs of acceptor and donor and B_{IH}(eV) is that between HOMOs of acceptor and donor, as shown in Figure 1. In the present study, the energy levels of each material are obtained from the literature.[17] It may be noted that the energy levels measured by different groups may vary influenced by the laboratory conditions and experimental accuracy. However, for our simulation model, we have carefully selected the values from the literature which give the best agreement with experimental results.

Considering the total solar power absorbed given in Equation (3) and all power losses as presented in Equation (4)–(7), the net maximum electrical power output, $P_{\text{net-max}}^{\text{Elect}}$, that can be harvested from an OSC:

$$\begin{aligned} P_{\text{net-max(OSC)}}^{\text{Elect}} &= Ir\alpha A - P_{\text{rec}} - P_{\text{B}} - P_{\text{BI}} - P_{\text{Thermal}} \\ &= P_{\text{G}} - P_{\text{rec}} - P_{\text{B}} - P_{\text{BI}} \end{aligned} \tag{8}$$

and for a PSC becomes:

$$P_{\text{net-max(PSC)}}^{\text{Elect}} = Ir\alpha A - P_{\text{rec}} - P_{\text{B}} - P_{\text{Thermal}} = P_{\text{G}} - P_{\text{rec}} - P_{\text{B}} \tag{9}$$

$P_{\text{net-max(OSC)}}^{\text{Elect}}$ and $P_{\text{net-max(PSC)}}^{\text{Elect}}$ in Equation (8) and (9) represent the net electrical power generated in the OSC and PSC,
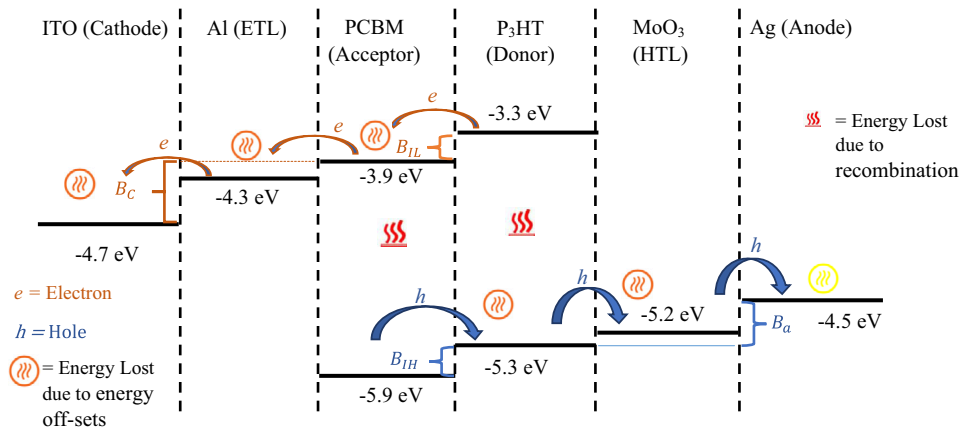
Figure 1. Schematic energy level alignment of functional materials used in the OSC of the structure: glass/indium tin oxide (ITO)/Al/poly (3-hexylthiophene) (P3HT):[6,6]-phenyl-C61-butyric acid methyl ester (PCBM)/molybdenum trioxide (MoO$_3$)/Ag.[17a-e]
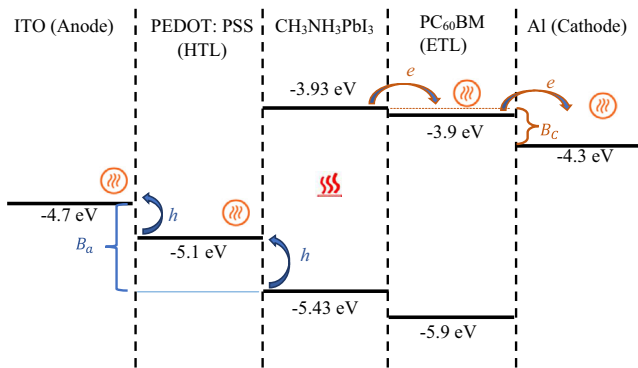
Figure 2. Schematic energy level alignment of functional materials used in the PSC of the structure: glass/ITO/poly(3,4-ethylenedioxythiophene): (polystyrene sulfuric acid) (PEDOT:PSS)/CH3NH3PbI3/PC60BM/Al.[17f–i]

respectively. Using these in Equation (1), PCE of both OSC and PSC can be written as:

$$PCE_{osc} = \frac{P^{Elect}_{net-max(OSC)}}{IrA} \quad (10)$$

and

$$PCE_{psc} = \frac{P^{Elect}_{net-max(PSC)}}{IrA} \quad (11)$$

One of the advantages of this approach is that it takes into account various possible power losses explicitly and hence provides insight into the influence of individual losses on PCE, which may not be possible to study experimentally.

3. Results and Discussions

To validate our simulation of PCE, we have considered two most studied solar cell structures: an OSC: glass/ITO/Al/ P$_3$HT: PCBM/MoO$_3$/Ag and a PSC: glass/ITO/ PEDOT: PSS/ CH$_3$NH$_3$PbI$_3$/PC$_{60}$BM/Al. Using the input data in **Table 1** and Equation (10) and (11), we have simulated PCE of both of the above OSC and PSC, as given in **Table 2**. We have also simulated PCE of both the structures using the conventional method and listed the results in Table 2 along with the corresponding experimental results.[18] Despite the relatively modest PCE observed in the two structures studied, their readily available input data make them suitable for accurate simulations. Furthermore, the simulation method can be extended to any OSC or PSC as long as their input parameters are known.

It may be noted that the values of all the fitting parameters listed in Table 1 are the best fit values to produce PCE in better agreement with their corresponding experimental results, as given in Table 2. The error in PCE obtained between the simulated results from Equation (10) and (11) and that of experiments is around 6.5% for OSC and 5.7% for PSC. It may also be desirable to know which of the input parameters listed in Table 1 have the most impact on PCE of each solar cell listed in Table 2. It is found through our simulation that the most significant influence on PCE of both OSC and PSC is due to the energy offset levels. Then the second most important parameter is the bandgap energy, and the third is the incident radiation. The variations in other parameters in Table 1 have only little influence on PCE of both solar cells.

It may be desirable to analyze the contribution of various power losses derived in Equation (2)–(7), to PCE of both OSC and PSC considered here. The contribution of P_G (Equation (3)) and P_{rec} (Equation (4)) on PCE of OSCs and PSCs is extensively covered in the literature.[8,19] However, to the best of the authors' knowledge, this is the first attempt to assess the contribution of P_B (Equation (5)) and P_{BI} (Equation (7)) on PCE of a solar cell. To get a better insight on the contribution of each power, P_G (Equation (3)), P_{rec} (Equation (4)), P_B (Equation (5)), and P_{BI} (Equation (3)), we have calculated their values for both OSC and PSC at the maximum power point (P_m). In this calculation, we have assumed the absorbance $\alpha = 0.6$ and $Ir = 1000 \, W \, m^{-2}$ at 1.5 AM. Each calculated power thus obtained is given in **Table 3**.

Table 1. List of input parameters used for the simulation in this paper.

Parameters	Value for OSC	Value for PSC
Ir [W m^{-2}] solar irradiance	1000 (standard condition)	1000 (standard condition)
G [s^{-1} m^{-3}] the rate of total electron-hole pair generation	6×10^{27}	6×10^{27}
B_a [eV] the energy offset between the anode and active layer	0.8[17a-e]	0.73[17f,g,i]
B_c [eV] the energy offset between the cathode and the active layer	0.8[17a-e]	0.37[17f,g]
B_{IL}[eV] is the energy offset between LUMOs of acceptor and donor	0.6[17a-e]	–
B_{IH}[eV] is the energy offset between HOMOs of acceptor and donor	0.6[17a-e]	–
α absorbance	0.6 (fitting parameter)	0.6 (fitting parameter)
T [K] solar cell temperature	298 (fitting parameter)	298 (fitting parameter)
E_g [eV] bandgap	2[17d,e,h]	1.6[17i]
d[nm)] active layer thickness	200	200
μ_n [m^2 V^{-1} s^{-1}] mobility of electrons	5×10^{-8} (fitting parameter)	10^{-4} (fitting parameter)
μ_p [m^2 V^{-1} s^{-1}] mobility of holes	10^{-8} (fitting parameter)	10^{-4} (fitting parameter)
N_{tInt}density of tail states at interface [cm^{-3} eV^{-1}]	10^{17} (fitting parameter)	10^{17} (fitting parameter)

Table 2. PCE obtained by our simulation and previous simulation work and from experiments for both OSC and PSC.

Solar cell	PCE obtained by the new simulation method [%]	PCE obtained by the conventional simulation method [%]	PCE obtained by experiment [%]
OSC	4.4%	4.7%	4.16[18a]
PSC	10%	11.3%	10.7[18b]

Table 3. The obtained values for P_G, P_{rec}, P_B, and P_{BI} for both OSC and PSC under P_m condition.

Parameters	OSC	PSC
$P_{Thermal}$ [W m^{-2}]	216	306
P_G [W m^{-2}]	384	294
P_{rec} [W m^{-2}]	165	53
P_B [W m^{-2}]	120	142
P_{BI} [W m^{-2}]	55	–
P_{net}^{Elect} [W m^{-2}]	44	99

According to Table 3, $P_{Thermal}$ is about 21.6% of the total incident power of 1000 W m^{-2} in OSC. After accounting $P_{Thermal}$, the total generated power P_G remains at 384 W m^{-2}, which is about 38.4% of the total incident power. Out of the total generated power, the power losses are $P_{rec} = 43\%$, $P_B = 31.3\%$, and $P_{BI} = 14.3\%$ of P_G. Thus, the remaining net output energy is 44 W m^{-2}, which is only 11.51% of P_G. Accordingly, the highest power loss occurs due to $P_{Thermal}$, followed by P_{rec}, P_B, and P_{BI} in OSC.

In the case of PSC, according to Table 3, $P_{Thermal}$ is 306 W m^{-2}, which is 30.6% of the incident irradiation power, $P_G = 294$ W m^{-2}, $P_{rec} = 53$ W m^{-2}, which is 18% of P_G and $P_B = 142$ W m^{-2}, about 48.3% of P_G. Thus, the net electrical power output obtained from PSC is 99 W m^{-2}, which is

33.7%. Here again, the maximum power loss in PSC is $P_{Thermal}$ followed by P_B and P_{rec}. No P_{BI} power loss is expected in PSC as free charge carriers not bound into excitons are excited due to the higher dielectric constant of perovskites.

4. Conclusion

In conclusion, this article introduces a new mathematical model to simulate PCE of an OSC and a PSC by incorporating all power losses that can occur before the charge carriers are collected by their respective electrodes. The validity of the mathematical model is tested by comparing the calculated PCE with the experimental results and the conventional simulation results, which are found in good agreement. Compared to conventional models, this model establishes a direct relationship between PCE and individual power losses that may occur in both OSCs and PSCs. The results show that the highest power loss occurs due to $P_{Thermal}$, followed by P_{rec}, P_B, and P_{BI} in OSC and the maximum power loss in PSC is $P_{Thermal}$ followed by P_B and P_{rec} in PSC.

Conflict of Interest

The authors declare no conflict of interest.

Data Availability Statement

The data that support the findings of this study are available from the corresponding author upon reasonable request.

Keywords

[1] H. M. Rad, M. Ameri, *Sol. Energy* **2016**, *132*, 570.

[2] a) K. Fukuda, K. Yu, T. Someya, *Adv. Energy Mater.* **2020**, *10*, 2000765; b) P. Roy, N. K. Sinha, S. Tiwari, A. Khare, *Sol. Energy* **2020**, *198*, 665.

[3] a) M. Ghorab, A. Fattah, M. Joodaki, *Optik* **2022**, *267*, 169730; b) M. Riede, D. Spoltore, K. Leo, *Adv. Energy Mater.* **2021**, *11*, 2002653; c) O. A. Abdulrazzaq, V. Saini, S. Bourdo, E. Dervishi, A. S. Biris, *Part. Sci. Technol.* **2013**, *31*, 427; d) D. Li, D. Zhang, K.-S. Lim, Y. Hu, Y. Rong, A. Mei, N.-G. Park, H. Han, *Adv. Funct. Mater.* **2021**, *31*, 2008621; e) N. Suresh Kumar, K. C. B. Naidu, *J. Mater.* **2021**, *7*, 940; f) T. Wu, Z. Qin, Y. Wang, Y. Wu, W. Chen, S. Zhang, M. Cai, S. Dai, J. Zhang, J. Liu, Z. Zhou, X. Liu, H. Segawa, H. Tan, Q. Tang, J. Fang, Y. Li, L. Ding, Z. Ning, Y. Qi, Y. Zhang, L. Han, *Nano-Micro Lett.* **2021**, *13*, 152.

[4] J. Fu, P. W. K. Fong, H. Liu, C.-S. Huang, X. Lu, S. Lu, M. Abdelsamie, T. Kodalle, C. M. Sutter-Fella, Y. Yang, G. Li, *Nat. Commun.* **2023**, *14*, 1760.

[5] a) H. Min, D. Y. Lee, J. Kim, G. Kim, K. S. Lee, J. Kim, M. J. Paik, Y. K. Kim, K. S. Kim, M. G. Kim, T. J. Shin, S. Il Seok, *Nature* **2021**, *598*, 444; b) N. R. E. Laboratory, Best Research-Cell Efficiency Chart, N. R. E. Laboratory **2024**, http://www.nrel.gov/pv/cell-efficiency.html.

[6] a) Beer, *Annalen der Physik* **1852**, *162*, 78; b) D. Ompong, M. Narayan, J. Singh, *J. Mater. Sci.: Mater. Electron.* **2017**, *28*, 7100.

[7] L. A. A. Pettersson, L. S. Roman, O. Inganäs, *J. Appl. Phys.* **1999**, *86*, 487.

[8] a) C. Liang, Y. Wang, D. Li, X. Ji, F. Zhang, Z. He, *Sol. Energy Mater. Sol. Cells* **2014**, *127*, 67; b) H. M. Rad, F. Zhu, J. Singh, *J. Appl. Phys.* **2018**, *124*, 083103.

[9] a) W. R. Frensley, University of Texas at Dallas **2004**, 1; b) H. K. Gummel, *IEEE Trans. Electron Devices* **1964**, *11*, 455; c) C. S. Rafferty, M. R. Pinto, R. W. Dutton, *IEEE Trans. Electron Devices* **1985**, *32*, 2018.

[10] a) X. Jia, H. An, Y. Hu, Z. Mo, *Comput. Math. Appl.* **2023**, *131*, 1; b) J. C. Meza, R. S. Tuminaro, *SIAM J. Sci. Comput.* **1996**, *17*, 118.

[11] E. H. dos Santos Rosa, E. L. Kowalski, L. F. R. B. Toledo, *Sol. Energy* **2021**, *221*, 483.

[12] K. S. Ram, D. Ompong, H. M. Rad, D. D. Y. Setsoafia, J. Singh, *Phys. Status Solidi* **2021**, *218*, 2000597.

[13] H. Mehdizadeh-Rad, K. Sreedhar Ram, F. Mehdizadeh-Rad, D. Ompong, D. D. Y. Setsoafia, N. K. Elumalai, F. Zhu, J. Singh, *Nanomaterials* **2022**, *12*, 420.

[14] H. Mehdizadeh-Rad, F. Mehdizadeh-Rad, F. Zhu, J. Singh, *Sol. Energy Mater. Sol. Cells* **2021**, *220*, 110837.

[15] a) D. Ompong, J. Singh, *ChemPhysChem* **2015**, *16*, 1281; b) C. M. Proctor, M. Kuik, T.-Q. Nguyen, *Prog. Polym. Sci.* **2013**, *38*, 1941.

[16] T. Kirchartz, B. E. Pieters, J. Kirkpatrick, U. Rau, J. Nelson, *Phys. Rev. B* **2011**, *83*, 115209.

[17] a) T. Hori, H. Moritou, N. Fukuoka, J. Sakamoto, A. Fujii, M. Ozaki, *Materials* **2010**, *3*, 4915; b) Y. Yin, D. A. Lewis, G. G. Andersson, *ACS Appl. Mater. Interfaces* **2018**, *10*, 44163; c) L. Lin, C. Gu, J. Zhu, Q. Ye, E. Jiang, W. Wang, M. Liao, Z. Yang, Y. Zeng, J. Sheng, W. Guo, B. Yan, P. Gao, J. Ye, Y. Zhu, *J. Mater. Sci.* **2019**, *54*, 7789; d) L. Safriani, R. Fitrilawati, M. Manawan, A. Bahtiar, A. Aprilia, D. P. Sari, J. Angel, I. Watanabe, *J. Phys.: Conf. Series* **2018**, *1080*, 012011; e) T. Wang, C. Chen, K. Guo, G. Chen, T. Xu, B. Wei, *Chin. Phys. B* **2016**, *25*, 038402; f) Z. Ku, Y. Rong, M. Xu, T. Liu, H. Han, *Sci. Rep.* **2013**, *3*, 3132; g) M. Z. Alotaibi, B. M. Omer, S. Alomairy, A. Merazga, *AIP Conf. Proc.* **2018** *1976*, 020010; h) M.-A. Pan, T.-K. Lau, Y. Tang, Y.-C. Wu, T. Liu, K. Li, M.-C. Chen, X. Lu, W. Ma, C. Zhan, *J. Mater. Chem. A* **2019**, *7*, 20713; i) M. Shirazi, M. R. Toroghinejad, R. Sabet Dariani, M. T. Hosseinnejad, *J. Mater. Sci.: Mater. Electron.* **2018**, *29*, 10092.

[18] a) Z. Kam, Q. Yang, X. Wang, B. Wu, F. Zhu, J. Zhang, J. Wu, *Org. Electron.* **2014**, *15*, 1306; b) K. Kim, B. Jung, N. Kumar, Y. Eom, W. Kim, *Phys. Status Solidi RRL* **2016**, *10*, 592.

[19] H. Mehdizadeh-Rad, J. Singh, *J. Mater. Sci.: Mater. Electron.* **2019**, *30*, 10064.

2300814 (5 of 5)